International Journal of Fracture, Vol. 18, No. 4, April 1982

The Hague, The Netherlands


# On localization in ductile materials containing spherical voids

VIGGO TVERGAARD

*Department of Solid Mechanics, The Technical University of Denmark, Lyngby, Denmark*

(Received May 16, 1980)

ABSTRACT

Macroscopic properties of a porous ductile medium are analysed on the basis of an axisymmetric numerical model and on the basis of a set of approximate constitutive equations for a voided material suggested by Gurson. Both models are used to analyse bifurcation into a localized mode. A number of predictions obtained by the two different approaches are in reasonable agreement; but it is found under several different loading conditions that the critical strain for localization is considerably overestimated by the approximate continuum model. A relatively simple modification of the constitutive equations for a voided medium results in considerably improved predictions.

## 1. Introduction

Microscopic voids in ductile materials play a crucial role in various fracture mechanisms. In some cases fracture is a direct consequence of the continued growth of voids with stretching, since finally the voids coalesce [1, 2, 3]. In other cases localization of the plastic deformations occurs before the general coalescence takes place. It has been shown by Rudnicki and Rice [4] and by Yamamoto [5] that a theory of plasticity, which accounts for the plastic dilatation that would be the overall effect of void growth, does predict significantly reduced critical strains for shear band instabilities.

In a recent paper [6] shear band instabilities in a void containing medium have been investigated by a numerical model that accounts in detail for the interaction between neighbouring voids and for the nonuniform stress field around each void. The computations in [6] were carried out for a material containing a doubly periodic array of circular cylindrical voids in the initial unstressed condition, which allows for the use of various symmetries in a plane strain solution. These predictions of shear band instabilities were compared with predictions based on the approximate constitutive equations for a voided ductile medium suggested by Gurson [7]. Good qualitative agreement was found and, based on this comparison, an adjustment of Gurson's constitutive relations was proposed. However, since the version of these constitutive equations that has been used is based on assuming spherical voids, a comparison with a numerical model for this void geometry is of considerable interest. The rapidly increasing number of applications of Gurson's model to study the influence of void growth on various failure mechanisms [5, 8–12] adds to the interest in an investigation of the accuracy that can be obtained by this continuum approximation.

Computations analogous to those in [6] are possible for an array of spherical voids periodic in three directions, but this would require three dimensional numerical solutions of the field equations. The investigations in the present paper are instead limited to configurations and load histories that can be analysed, at least approximately, in terms of an axisymmetric model problem. This model does not

0376-9429/82/040237-16$00.20/0

facilitate analyses of localization into shear bands of arbitrary inclination to the maximum principal stress direction; but the special case of bands perpendicular to this direction is easily accounted for. A few results obtained by a spherically symmetric model are presented as well.

In an actual material most of the voids are nucleated during the plastic deformation, when second phase particles crack or debond from the surrounding matrix. However, the analyses in the present paper rely on the simplifying assumption that all voids are initially present in the material. This approximation will be reasonable in a number of cases, in which the voids of interest nucleate at a very early stage of the deformation.

## 2. Axisymmetric model problem

The model to be used here for studying the influence of spherical voids in a ductile medium is an axisymmetric model, as shown in Fig. 1. The voids of initial radius $R_0$ are taken to be located along the axis of a circular cylindrical body with an initial spacing $2B_0$ between the centres. The cylindrical body has an initial radius $A_0$, and the surface of this body is taken to remain cylindrical throughout the deformation. Thus, in the direction perpendicular to the $x^3$-axis this axisymmetric model may be considered an approximation of a hexagonal cell in the void distribution sketched in Fig. 1b, where an initial distance $\sqrt{2\pi/\sqrt{3}}A_0$ between neighbouring void centres corresponds to the initial void volume fraction in the cylindrical body. Due to symmetries only the region hatched in Fig. 1a needs be accounted for in the axisymmetric analysis of the deformation history.

A Lagrangian formulation of the field equations is used, with reference to a cylindrical coordinate system, in which $x^1$ is the radius, $x^2$ is the circumferential angle, and $x^3$ is the axial coordinate. The displacement components relative to the reference

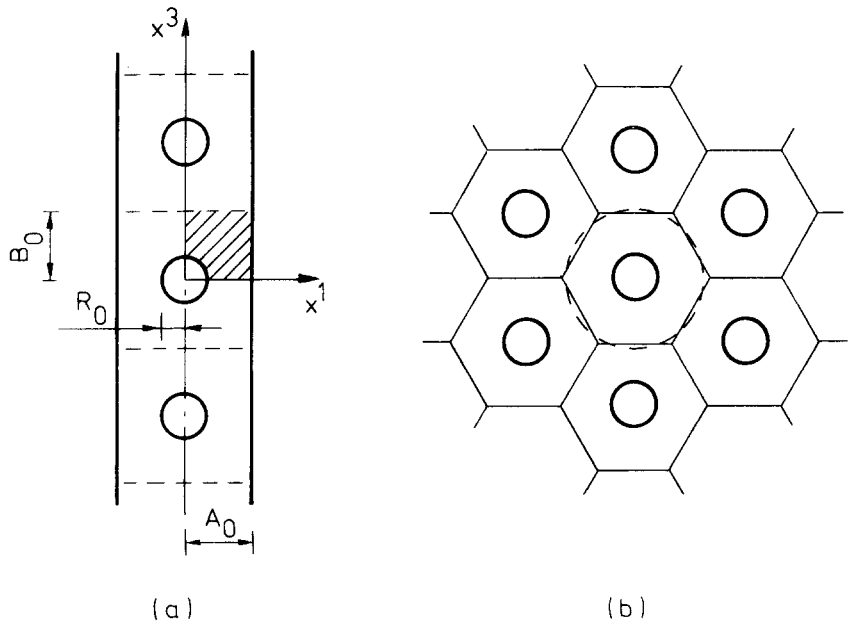


Figure 1. Axisymmetric model of a material containing spherical voids.

coordinate system are $u^i$ and the Lagrangian strain increments are given by

$$\dot{\eta}_{ij} = \tfrac{1}{2}(\dot{u}_{i,j} + \dot{u}_{j,i} + \dot{u}^k{}_{,i}u_{k,j} + u^k{}_{,i}\dot{u}_{k,j}) \tag{2.1}$$

where $(\,)_{,i}$ denotes covariant differentiation in the reference configuration and $(\dot{})$ denotes differentiation with respect to a loading parameter. The contravariant components $\tau^{ij}$ of the Kirchhoff stress tensor on the embedded deformed coordinates are related to the Cauchy stress tensor $\sigma^{ij}$ by

$$\tau^{ij} = \sqrt{G/g}\,\sigma^{ij} \tag{2.2}$$

Here, $g$ and $G$ are the determinants of the metric tensors $g_{ij}$ and $G_{ij}$ in the reference configuration and in the current configuration, respectively.

The equilibrium equations are written in the form of the incremental principle of virtual work

$$\int_V \{\dot{\tau}^{ij}\delta\dot{\eta}_{ij} + \tau^{ij}\dot{u}^k{}_{,i}\delta\dot{u}_{k,jk,j}\}\,\mathrm{d}V = \int_S \dot{T}^i\delta\dot{u}_i\,\mathrm{d}S \tag{2.3}$$

where the volume and surface of the body in the reference configuration are denoted by $V$ and $S$, respectively, and the nominal traction increments on a surface with reference normal $n_j$ are given by

$$\dot{T}^i = (\dot{\tau}^{ij} + \dot{\tau}^{kj}u^i{}_{,k} + \tau^{kj}\dot{u}^i{}_{,k})n_j \tag{2.4}$$

As in [6] a large strain generalisation of $J_2$ flow theory is used for the elastic–plastic material behaviour, with an incremental stress strain relation of the form

$$\dot{\tau}^{ij} = L^{ijkl}\dot{\eta}_{kl} \tag{2.5}$$

The expression for the instantaneous moduli $L^{ijkl}$ shall not be repeated here. The uniaxial stress–strain curve that defines the tangent modulus at a given level of the effective Mises stress is taken to be given by

$$\epsilon = \begin{cases} \dfrac{\sigma}{E}, & \text{for } \sigma \leq \sigma_y \\[2ex] \dfrac{\sigma_y}{E}\left(\dfrac{\sigma}{\sigma_y}\right)^n, & \text{for } \sigma > \sigma_y \end{cases} \tag{2.6}$$

where $\epsilon$ is the logarithmic strain, $\sigma$ is the true stress, $E$ is Young's modulus, $\sigma_y$ is the uniaxial yield stress, and $n$ is the strain hardening exponent.

The boundary conditions specified for the axisymmetric region considered are

$$\dot{T}^i = 0, \quad \text{at } (x^1)^2 + (x^3)^2 = R_0^2 \tag{2.7}$$

$$\dot{u}^3 = 0, \qquad \dot{T}^1 = \dot{T}^2 = 0, \quad \text{at } x^3 = 0 \tag{2.8}$$

$$\dot{u}^3 = \dot{U}_{\mathrm{III}}, \qquad \dot{T}^1 = \dot{T}^2 = 0, \quad \text{at } x^3 = B_0 \tag{2.9}$$

$$\dot{u}^1 = \dot{U}_{\mathrm{I}}, \qquad \dot{T}^2 = \dot{T}^3 = 0, \quad \text{at } x^1 = A_0 \tag{2.10}$$

where the two constants $\dot{U}_{\mathrm{I}}$ and $\dot{U}_{\mathrm{III}}$ are displacement increments to be prescribed. The corresponding average nominal traction increments in axial and radial direction, respectively, are given by integrals along the surfaces

$$\dot{T}_{\mathrm{I}} = \frac{1}{B_0}\int_0^{B_0} [\dot{T}^1]_{x^1=A_0}\,\mathrm{d}x^3, \qquad \dot{T}_{\mathrm{III}} = \frac{2}{A_0^2}\int_0^{A_0} [\dot{T}^3 x^1]_{x^3=B_0}\,\mathrm{d}x^1 \tag{2.11}$$

Now, in the present investigation we choose to focus on situations in which the ratio of the average true stresses $\sigma_1$ and $\sigma_3$ perpendicular to the axis and in the axial

direction, respectively, is a constant $\rho$

$$\sigma_1/\sigma_3 = \dot{\sigma}_1/\dot{\sigma}_3 = \rho \tag{2.12}$$

while the axial displacement $U_{III}$ grows monotonically. Introducing the current dimensions $A = A_0 + U_I$ and $B = B_0 + U_{III}$ of the region considered, the stresses are given by $\sigma_1 = T_I A_0 B_0 (AB)^{-1}$ and $\sigma_3 = T_{III} A_0^2 A^{-2}$, and the incremental form of (2.12) can be written as

$$\dot{T}_I = \rho \frac{A_0}{B_0}\left[\dot{T}_{III}\frac{B}{A} + T_{III}\frac{\dot{B}}{A} - T_{III}\frac{B\dot{A}}{A^2}\right] \tag{2.13}$$

Thus, in solving the incremental equilibrium equations (2.3) with the boundary conditions (2.7)–(2.10) the ratio between $\dot{U}_I = \dot{A}$ and $\dot{U}_{III} = \dot{B}$ is determined by (2.11) and (2.13), so that (2.12) is satisfied.

Localization into a band perpendicular to the $x^3$-axis requires, according to a standard shear band analysis (see for example [6]), that a slice of material can undergo an increment of deformation different from that in the surrounding material. In the following the difference between an increment of the bifurcation mode and the corresponding increment of the fundamental mode is denoted by $(\tilde{\ })$. Now, localization in a band limited by $x^3 = 0$ and $x^3 = B_0$ occurs, if a solution increment $\tilde{u}_i$ satisfies the incremental equilibrium equation (2.3) and the boundary conditions (2.7)–(2.10), with $(\dot{\ })$ replaced by $(\tilde{\ })$ everywhere, for $\tilde{U}_I = 0$ and for the two conditions $\tilde{U}_{III} \neq 0$, $\tilde{T}_{III} = 0$ satisfied simultaneously. However, with $\tilde{u}_{i,j} \equiv 0$ outside the band, this mode would only on the average satisfy compatibility of the radial displacement increments $\tilde{u}_1$ on the band interfaces.

A rather similar bifurcation mode, illustrated in Fig. 2, is one that strictly satisfies compatibility and equilibrium together with all the prescribed boundary conditions (2.7)–(2.13), except that the symmetry condition (2.9) is replaced by the corresponding symmetry condition at $x^3 = 2B_0$. This bifurcation mode is antisymmetric about $x^3 = B_0$. Thus for the region considered (hatched in Fig. 1a) the symmetry condition (2.9) is replaced by the following condition of antisymmetry

$$\tilde{u}^1 = 0, \qquad \tilde{T}^2 = \tilde{T}^3 = 0, \quad \text{at } x^3 = B_0 \tag{2.14}$$

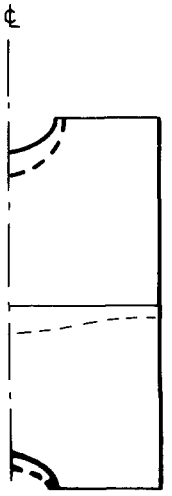


Figure 2. Bifurcation mode for axisymmetric void model indicated by dotted lines. The current state of deformation before bifurcation is shown by solid lines.

This eigenmode, in which some layers of voids are being compressed and the neighbouring layers are being expanded, occurs without additional overall straining and without changes of the average stresses, $\tilde{U}_{\mathrm{I}} = \tilde{U}_{\mathrm{III}} = 0$ and $\tilde{T}_{\mathrm{I}} = \tilde{T}_{\mathrm{III}} = 0$ for a cell enclosed by $x^1 = A_0$ and $x^3 = 0, 2B_0$. The bifurcation analysis is based on the general theory of Hill [13], and is carried out as described in [6].

Both the above mentioned bifurcation analyses are applied to each case considered, and for all the results to be presented in Section 4 the critical strains predicted by the two analyses are virtually identical.

## 3. Continuum model of a ductile porous medium

An approximate continuum representation of the response of a ductile void-containing material can be obtained by accounting for the plastic dilatancy that will be the apparent macroscopic effect of void growth. This was already suggested by Berg [14], and subsequently various authors have included plastic dilatancy into elastic–plastic constitutive equations. Of particular interest are the approximate constitutive equations proposed by Gurson [7, 15], since here modifications of the classical Prandtl–Reuss equations, dependent on the current void volume fraction, have been specified in detail, on the basis of approximate rigid-perfectly plastic computations for special void geometries. This set of equations has already been used in a number of investigations of the influence of voids on various fracture mechanisms [5, 8–12].

Gurson's equations are formulated in terms of the average macroscopic Cauchy stress tensor $\sigma^{ij}$, with the corresponding stress deviator $s^{ij} = \sigma^{ij} - G^{ij}\sigma^k_k/3$ and effective Mises stress $\sigma_e = (3s_{ij}s^{ij}/2)^{1/2}$. The actual microscopic stress state in the matrix material is represented by the equivalent tensile flow stress $\sigma_M$. The approximate yield condition

$$\Phi = \frac{\sigma_e^2}{\sigma_M^2} + 2fq_1 \cosh\left\{\frac{q_2}{2}\frac{\sigma^k_k}{\sigma_M}\right\} - (1 + q_3 f^2) = 0 \tag{3.1}$$

in which $f$ is the current void volume fraction, is that suggested by Gurson (for $q_1 = q_2 = q_3 = 1$) based on spherically symmetric deformations around a single spherical void. The additional adjustable parameters $q_i$ in (3.1) were introduced in [6].

It may be noted that alternative yield conditions $\Phi(\sigma^{ij}, \sigma_M, f) = 0$ could be used, such as the conditions suggested by Gurson [7] on the basis of axisymmetric flow around cylindrical voids or on the basis of plastic flow with rigid sections near each void. However, here we shall concentrate on the yield condition of the form (3.1), which has been used so far in all applications of this continuum model.

In Gurson's model the increment $\dot{\epsilon}^P_M$ of the effective plastic strain in the matrix material is assumed to satisfy the following two relations

$$\dot{\epsilon}^P_M = \left(\frac{1}{E_t} - \frac{1}{E}\right)\dot{\sigma}_M, \qquad \sigma^{ij}\dot{\eta}^P_{ij} = (1-f)\sigma_M\dot{\epsilon}^P_M \tag{3.2}$$

where $E_t$ is the current tangent modulus in the matrix material and $\eta^P_{ij}$ is the plastic part of the macroscopic Lagrangian strain tensor. Thus, the increment of $\sigma_M$ is given by

$$\dot{\sigma}_M = \frac{EE_t}{E - E_t}\frac{\sigma^{ij}\dot{\eta}^P_{ij}}{(1-f)\sigma_M} \tag{3.3}$$

Obviously, the quantities $\sigma_M$, $\epsilon_M$ and $E_t$ can only represent some average of the field quantities in the matrix, since the actual stress state around the voids is strongly nonhomogeneous.

The increment of the current void volume fraction is given by the expression

$$\dot{f} = (1-f)G^{ij}\dot{\eta}^P_{ij} \tag{3.4}$$

since the matrix material is taken to be plastically incompressible. Furthermore, the argument is used [14, 7] that normality for the matrix material implies macroscopic normality

$$\dot{\eta}^P_{ij} = \Lambda \frac{\partial \Phi}{\partial \sigma^{ij}} \tag{3.5}$$

The parameter $\Lambda$ is determined from the consistency condition $\dot{\Phi} = 0$, required for continued plastic loading. The detailed expressions are shown in [6], including the expression for the tensor of instantaneous moduli $L^{ijkl}$ to be used in the constitutive equation of the form (2.5).

It is of interest to note that, independent of the additional parameters $q_i$, the constitutive relations based on (3.1) and the following equations reduce to the equations of $J_2$ flow theory in the limit $f = 0$. This is consistent with the use of $J_2$ flow theory in the numerical model of Section 2.

Bifurcation in a shear band mode occurs when deformations different from the otherwise homogeneous state of deformation are possible in a thin slice of material. Such bifurcation coincides with loss of ellipticity of the governing differential equations. Here, the conditions for shear band formation shall be given quite briefly, with reference to a Cartesian coordinate system, and with quantities inside and outside the band denoted by $(\ )^b$ and $(\ )^0$, respectively. Compatibility requires zero jump in tangential derivatives of $\dot{u}_i$ over the band interface, as expressed by the equations

$$\dot{u}^b_{i,j} - \dot{u}^0_{i,j} = n_j c_i \tag{3.6}$$

in which $n_j$ is the normal of the band and $c_i$ are parameters to be determined. Substituting (3.6) into the equilibrium requirement of equal tractions on the two sides of the band interface

$$\dot{T}^i_b - \dot{T}^i_0 = 0 \tag{3.7}$$

using (2.4), (2.5) and (2.1), leads to the three homogeneous algebraic equations for $c_i$ that govern bifurcation.

## 4. Results for axisymmetric model

In the examples to be considered here the initial void volume fraction is denoted by $f_0$. For the Gurson model this one parameter is the only specification of the voids, whereas for the axisymmetric model problem described in Section 2 the initial geometry is specified in more detail by $R_0$, $A_0$ and $B_0$, and in terms of these dimensions the initial void volume fraction is $f_0 = 2R_0^3(3A_0^2B_0)^{-1}$. In the cases considered in Fig. 3, with $B_0/A_0 = 1$, the void dimensions $R_0/A_0 = 0.25$, 0.30, 0.35 and 0.40 correspond to $f_0 = 0.0104$, 0.018, 0.0286 and 0.0427, respectively.

The numerical solutions for the axisymmetric model problem are obtained by a linear incremental method based on finite element approximations of the displacement increments in terms of eight-noded isoparametric elements. The mesh used for the hatched area in Fig. 1a is identical to that used in the plane strain computations of [6], with 4 elements along lines through the void centre and 6 elements along the quarter circle. Computations with a finer mesh and with a cruder mesh indicate that the solutions obtained by this $4 \times 6$ mesh are sufficiently accurate.

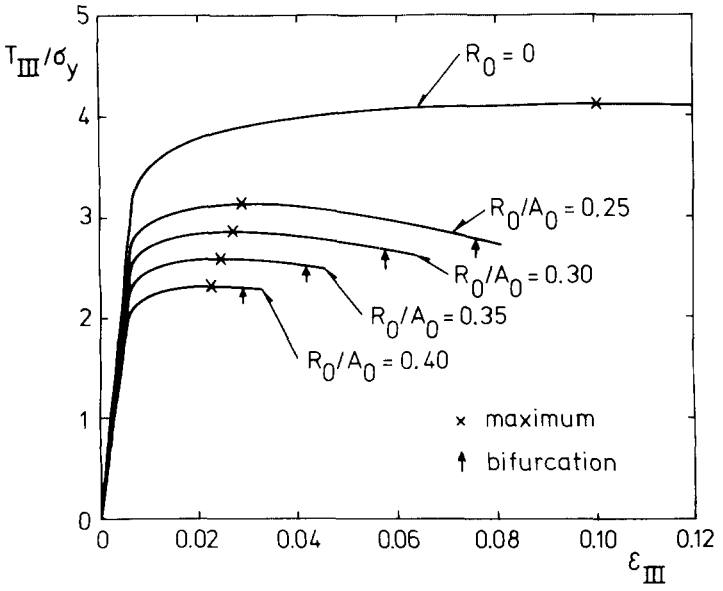


Figure 3. Nominal traction versus average strain for $\rho = 0.7$ and $B_0/A_0 = 1$. Matrix material characterized by $\sigma_y/E = 0.004$, $n = 10$ and $\nu = 1/3$.

For the material considered in Fig. 3 the initial yield stress is specified by $\sigma_y/E = 0.004$, Poisson's ratio is $\nu = 1/3$ and the strain hardening exponent is $n = 10$. Furthermore, the stress ratio (2.12) is taken to be $\rho = \sigma_1/\sigma_3 = 0.7$. The figure shows a plot of the nominal traction $T_{III}$ in the axial direction versus the axial logarithmic strain $\epsilon_{III} = \log(1 + U_{III}/B_0)$. Clearly, the strain at which the maximum load occurs is strongly reduced by the presence of voids and also the maximum loads are somewhat reduced. Furthermore, in the range considered the critical strain for bifurcation is very sensitive to the initial void volume fraction.

In Fig. 4 the numerical results of the previous figure are compared with predictions of the approximate constitutive relations. The predictions based on the yield function originally proposed by Gurson ($q_1 = q_2 = q_3 = 1$ in (3.1)) are shown by solid curves, while the dashed curves correspond to the set of parameters $q_1 = 1.5$, $q_2 = 1$ and $q_3 = q_1^2$ that was also chosen in [6]. No attempt has been made here to determine the set of parameters $q_i$ that give the best agreement with the numerical results of the axisymmetric model problem. However, the comparison with predictions based on the two different sets of parameters in (3.1) gives a useful indication of the accuracy that can be obtained by the Gurson model. In the following the two different choices of parameters are indicated by $q_1 = 1$ and $q_1 = 1.5$, respectively.

The quantities compared in Fig. 4a are the maximum nominal traction $T_{III}$ and the corresponding strain $\epsilon_{III}$ in the axial direction, for various initial void volume fractions $f_0$. In Fig. 4b the critical strains and corresponding tractions are compared for localization into a band perpendicular to the maximum principal stress direction. The most drastic difference in Fig. 4 is that of the critical bifurcation strains, where the strains predicted by the unmodified Gurson model are far too large, whereas the predictions of the modified model are considerably closer and could be still better if a larger value of $q_1$ was chosen. Neither of the traction comparisons show a clear preference of any of the two curves, and regarding the strains at the maximum the agreement with the dashed curve is only slightly better than with the solid curve. Note

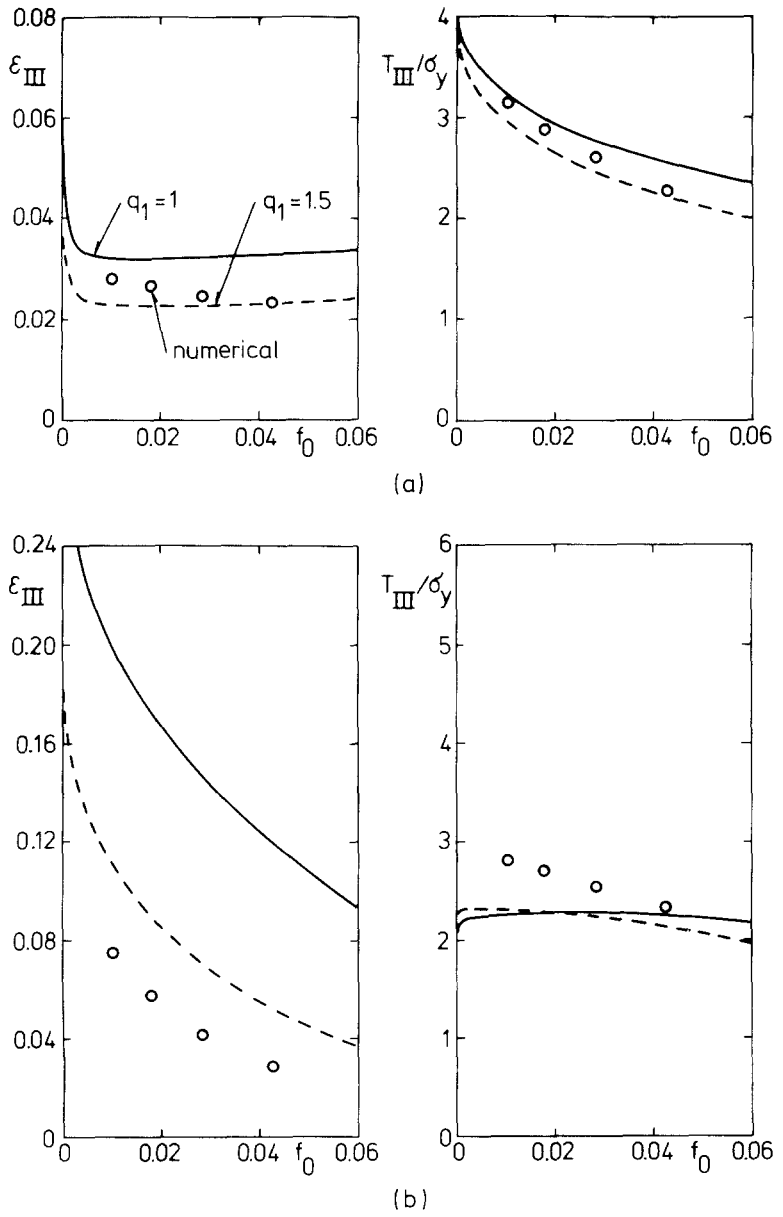


Figure 4. Axial strains and tractions versus initial void volume fraction $f_0$ computed numerically for $\rho = 0.7$ and $B_0/A_0 = 1$ and by continuum model (curves). (a) Values at maximum axial load. (b) Values at bifurcation. Matrix material characterized by $\sigma_y/E = 0.004$, $n = 10$ and $\nu = 1/3$.

that the strains at the maximum are strongly sensitive to very small void volume fractions.

In Fig. 5a the corresponding comparison is made of the total material dilatancy for various initial void volume fractions. The volume increase $\Delta V$ plotted here for $\epsilon = 0.04$, 0.08 and 0.12, respectively, is mainly due to void growth, but includes also elastic volume changes. It is seen that the dilatancy and thus the void growth in the numerical model is considerably better approximated by the modified version of Gurson's equations than by the unmodified version. This may partly explain the strong delay of the bifurcation predicted by the solid curve in Fig. 4b, since an underestimate

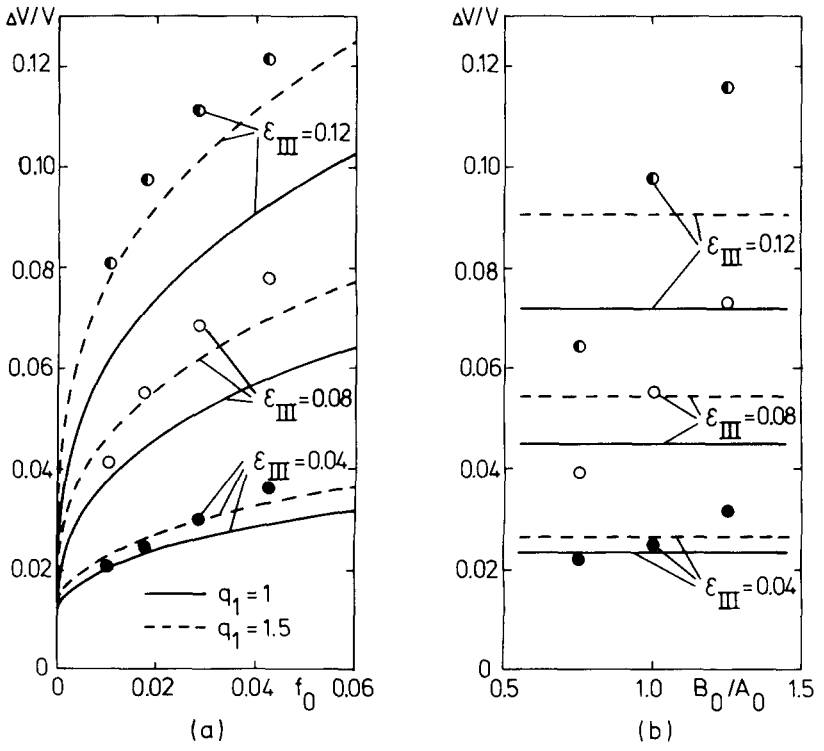


Figure 5. Dilatancy at various levels of axial strain computed numerically for $\rho = 0.7$ and by continuum model (curves). (a) $B_0/A_0 = 1$ and varying initial void volume fraction. (b) $f_0 = 0.018$ and varying dimensions $B_0/A_0$. Matrix material characterized by $\sigma_y/E = 0.004$, $n = 10$ and $\nu = 1/3$.

of the void growth also results in an underestimate of the corresponding material softening. However, another reason for this discrepancy may be the interaction between neighbouring voids, which results in highly strained zones that link up the voids. Due to the strongly nonlinear material behaviour these highly strained zones may soften the macroscopic material response, and thus lead to earlier localization.

It is also of interest to see how the initial void configuration affects the material response for a given void volume fraction, since such a dependence is not accounted for in the approximate constitutive equations for the porous medium. Therefore, in Fig. 5b and in Fig. 6 the ratio $B_0/A_0$ is varied and the initial void radius $R_0$ is varied simultaneously, such that the initial void volume fraction remains constant, $f_0 = 0.018$. The figures show that in fact, both the dilatancy, the strain at the maximum load and the bifurcation strain vary considerably with $B_0/A_0$. This does represent a noteworthy limitation on the accuracy that can be obtained by the approximate constitutive equations; but still the constitutive equations with $q_1 = 1.5$ appear to give the better approximation.

In Fig. 7 the stress ratio $\rho = \sigma_1/\sigma_3$ in (2.12) and (2.13) is varied for a fixed initial void volume fraction, $f_0 = 0.018$. The strain at the maximum load increases rather strongly for decreasing $\rho$ in a range around $\rho = 0.6$; but for smaller $\rho$ (not shown in the figure) the curves flatten out leading to $\epsilon_{III} \simeq 0.1$ at the maximum for uniaxial tension. As in the previous figures the agreement between numerical and continuum theory results is rather good at the maximum (Fig. 7a) and less good at bifurcation (Fig. 7b), with the better agreement for $q_1 = 1.5$ in the continuum approach.

The bifurcation strains compared in Fig. 7b and in all the previous figures are

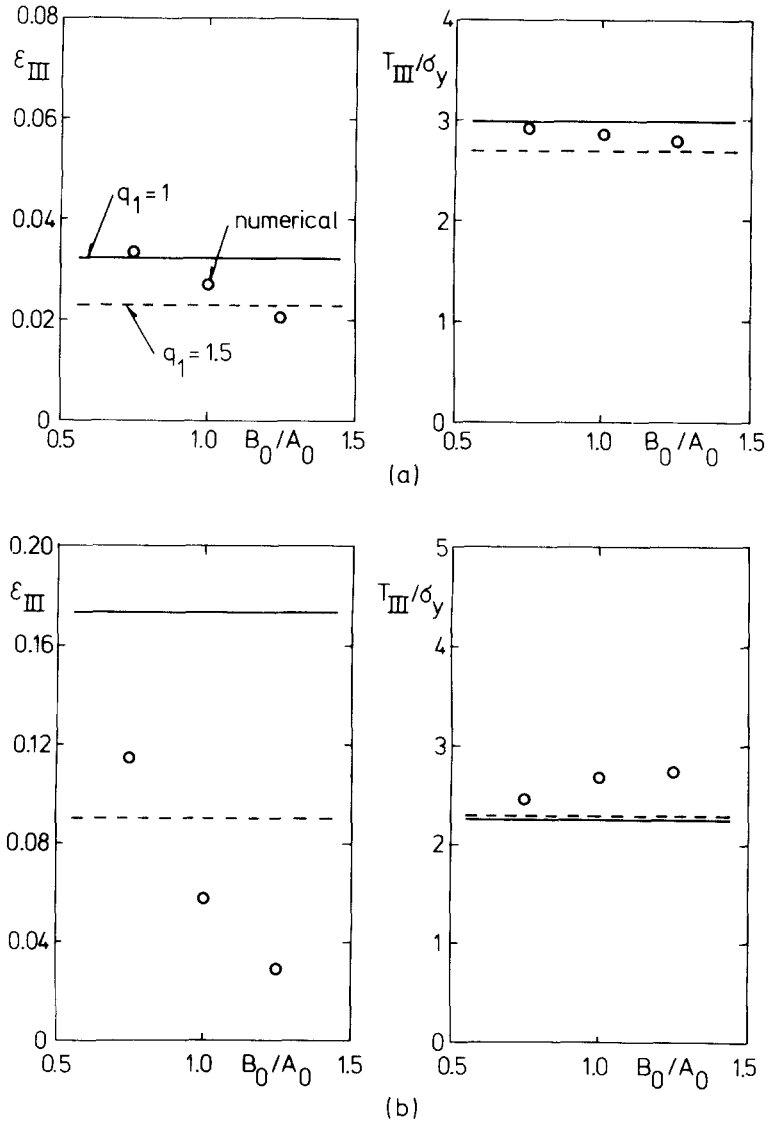


Figure 6. Axial strains and tractions versus $B_0/A_0$ computed numerically for $f_0 = 0.018$ and $\rho = 0.7$ and by continuum model (curves). (a) Values at maximum axial load. (b) Values at bifurcation. Matrix material characterized by $\sigma_y/E = 0.004$, $n = 10$ and $\nu = 1/3$.

those corresponding to localization in a band with an angle of inclination $\psi = 0°$ between the normal vector and the $x^3$ axis. This is the only type of mode discussed in Section 2 for the axisymmetric model problem. However, the inclination of the shear band that is first critical is usually different from zero, and therefore the approximate constitutive equations have been used to compute the critical shear band bifurcations and the corresponding inclinations, as shown in Fig. 8. It is seen that around $\rho = 0.85$ there is a small interval, in which $\psi = 0°$ is actually the critical inclination. Furthermore, comparison with Fig. 7b shows that, even when the critical inclination is around 20°, bifurcation in the critical mode occurs only slightly before the mode with $\psi = 0°$. Both Fig. 7b and Fig. 8 show that the bifurcation strains grow rapidly for decreasing $\rho$. In uniaxial tension ($\rho = 0$) localization in a shear band requires very large prestrains.

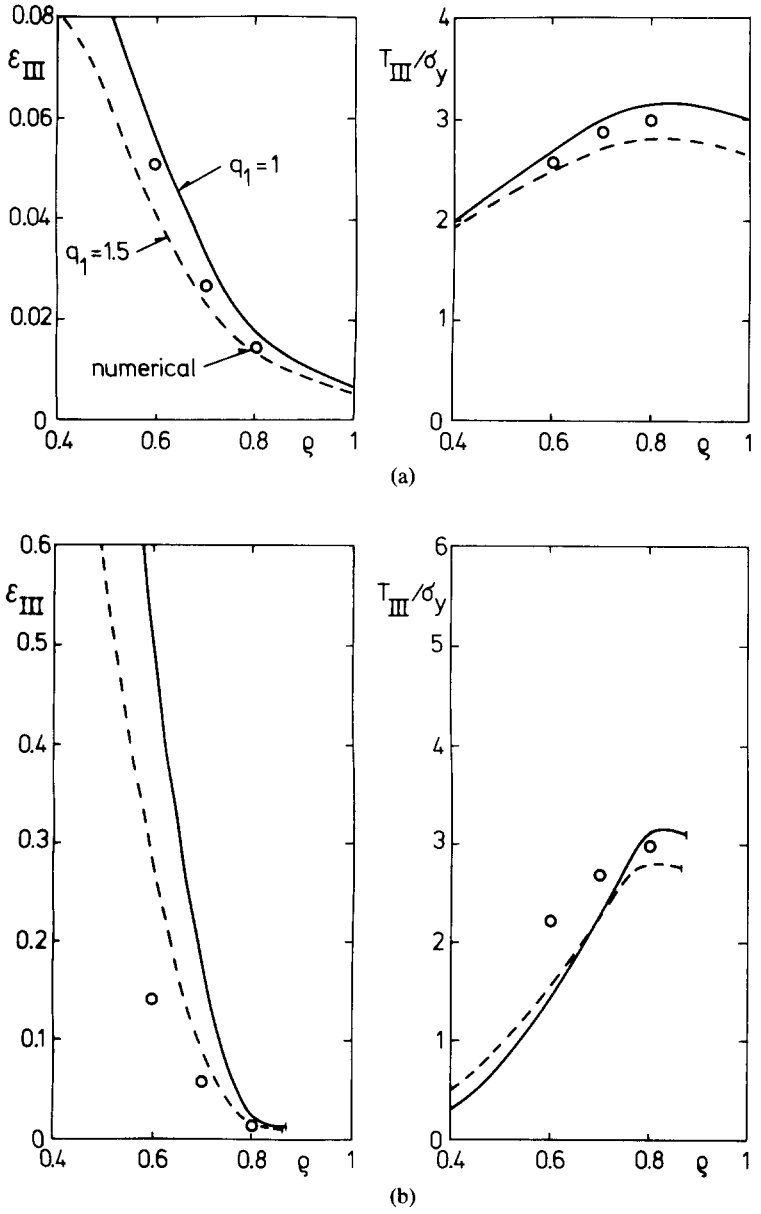


Figure 7. Axial strains and tractions versus stress ratio $\rho$ computed numerically for $f_0 = 0.018$ and $B_0/A_0 = 1$ and by continuum model (curves). (a) Values at maximum axial load. (b) Values at bifurcation. Matrix material characterized by $\sigma_y/E = 0.004$, $n = 10$ and $\nu = 1/3$.

On the other hand for $\rho$ close to unity, where all principal strains are positive, no bifurcation is found.

Finally, in Fig. 9 the effect of varying the strain hardening exponent $n$ is studied for a fixed initial void volume fraction $f_0 = 0.018$ and stress ratio $\rho = 0.7$. The sensitivity of the bifurcation strain to varying $n$ is somewhat underestimated by the Gurson model, which is opposite to the tendency found by comparison with the numerical results for cylindrical voids [6]. However, the variation of the maximum load and the corresponding strain is well represented by this continuum theory.

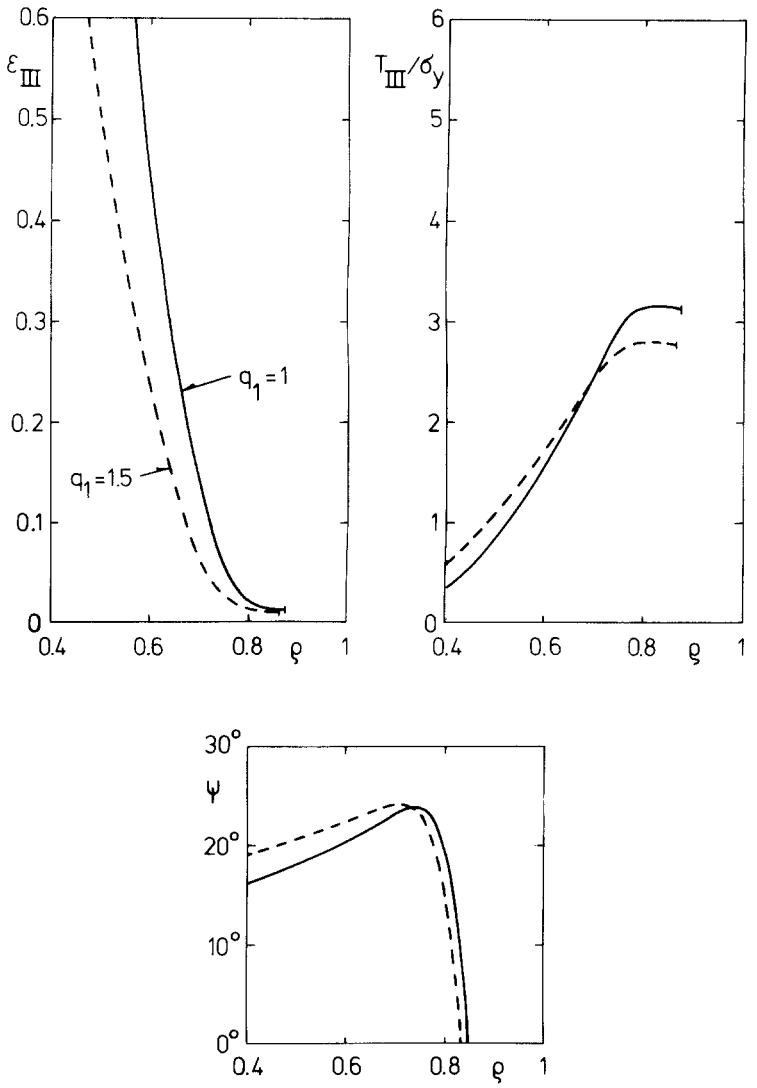


Figure 8. Axial strains and tractions at bifurcation into shear bands with the critical angle of inclination $\psi$. Continuum model predictions versus stress ratio $\rho$ for $f_0 = 0.018$. Matrix material characterized by $\sigma_y/E = 0.004$, $n = 10$ and $\nu = 1/3$.

## 5. Spherically symmetric model problem

The simplest among the models that can be used to obtain an estimate of the response of a void containing ductile medium is that of spherically symmetric deformation around a spherical void. This model requires only a one dimensional analysis; but, in contrast to the axisymmetric model of Section 2 and the plane strain analysis for cylindrical voids in [6], the spherically symmetry model can only give an estimate of the behaviour under purely hydrostatic loading. This model was in fact the one used by Gurson [7], assuming rigid-perfectly plastic material behaviour, to derive the approximate initial yield condition (3.1).

Here, the comparisons shown in the previous Figs. 4–9 shall be concluded by a few results obtained for this spherical model, on the basis of a strain hardening elastic

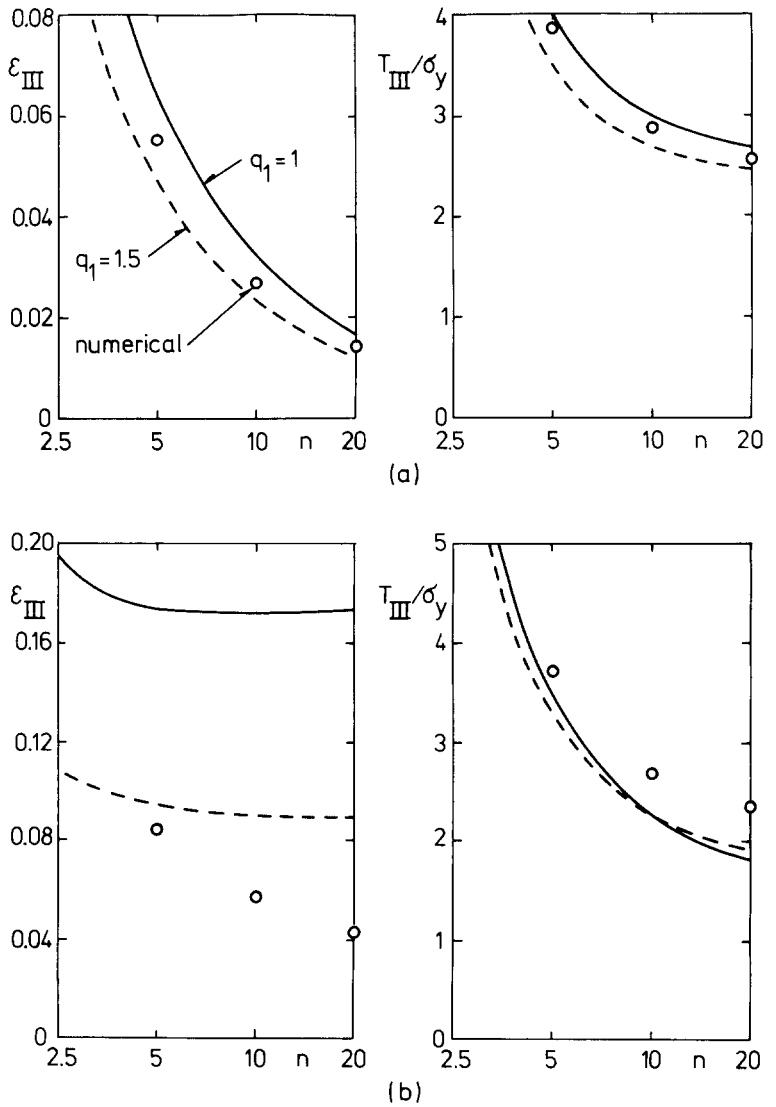


Figure 9. Axial strains and tractions versus strain hardening exponent $n$ computed numerically for $f_0 = 0.018$, $\rho = 0.7$ and $B_0/A_0 = 1$ and by continuum model (curves). (a) Values at maximum axial load. (b) Values at bifurcation. Matrix material characterized by $\sigma_y/E = 0.004$ and $\nu = 1/3$.

plastic material. The spherical body has an initial radius $C_0$, the initial radius of the concentric spherical void is $R_0$, and thus the model may be considered approximately representative of a solid with an initial void volume fraction $f_0 = (R_0/C_0)^3$. The macroscopic response of this solid is represented by the variation of the nominal traction $T$ on the surface versus the true strain of the radius $\epsilon = \log(1 + \Delta C/C_0)$. The programme used to compute this relationship is described in [16].

In Figs. 10a and b the initial void volume fractions are $f_0 = 0.01$ and $f_0 = 0.03$, respectively, in a material with strain hardening exponent $n = 10$. Comparison with predictions of the continuum model of a voided material shows that in this case of hydrostatic tension ($\rho = 1$ in (2.12)) the unmodified version of (3.1), originally suggested by Gurson [7], gives the better agreement with the numerical results for the spherical body. However, both for $q_1 = 1$ and for $q_1 = 1.5$ the curves are clearly

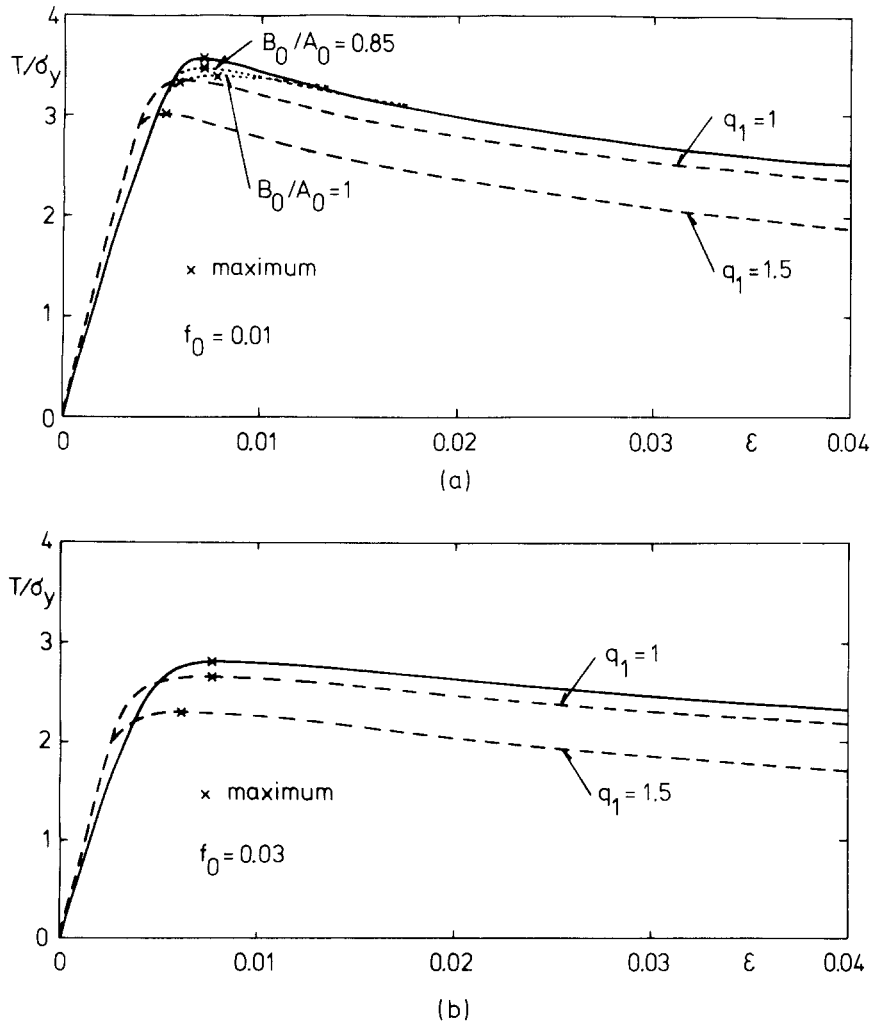


Figure 10. Nominal traction versus strain under hydrostatic tension as predicted by spherically symmetric model (solid curves), by continuum model (dashed curves) and by axisymmetric numerical model (dotted curves). Matrix material characterized by $\sigma_y/E = 0.004$, $n = 10$ and $\nu = 1/3$.

parallel with that obtained numerically. The deviations between the initial parts of the curves depend on the fact that in the actual spherical model yielding starts at the void surface for $T/\sigma_y \approx 0.8$ and reaches the external surface around the maximum load, whereas in the continuum approximations yielding occurs everywhere simultaneously, when the yield condition (3.1) is satisfied.

A few results computed by the axisymmetric model of Section 2 are included in Fig. 10a. In these cases the values plotted are those in axial direction, $T_{III}/\sigma_y$ versus $\epsilon_{III}$, since in the axisymmetric model there is no guarantee that hydrostatic tension ($\rho = 1$ in (2.12)) will result in uniform principal strains. Thus, for $B_0/A_0 = 1$ the axial strain $\epsilon_{III}$ grows considerably faster than the transverse strain $\epsilon_I$, already before the maximum is reached, and therefore this curve starts to rapidly deviate from that obtained by the spherical model. Better agreement is found for $B_0/A_0 = 0.85$, but even here the principal strains deviate increasingly after the maximum. If an average strain measure $\epsilon = \frac{1}{3}\log(1 + \Delta V/V)$ based on the volume increase $\Delta V$ is used instead of $\epsilon_{III}$ for these plots, both results of the axisymmetric model come out much closer to parallel with the solid curve in Fig. 10a. On

the other hand, equality of the macroscopic principal strains is an inherent part of the spherical model, and in the continuum model the same equality results for $\sigma_I = \sigma_{II} = \sigma_{III}$, due to the effective isotropy of the constitutive relations. It may be noted that in the results of Section 4 the agreement of strain ratios predicted by the different models for a given prescribed stress ratio is checked by the plots of dilatations versus axial strains shown in Fig. 5.

## 6. Concluding remarks

The comparisons made in the present paper for spherical voids and previously for cylindrical voids under plane strain conditions indicate that the approximate constitutive equations for a ductile porous material suggested by Gurson provide a very useful basis for estimating the influence of void growth on material behaviour. Under the conditions of hydrostatic tension that formed the basis of Gurson's approximate macroscopic yield criterion the behaviour is well predicted by this continuum approach. Also for various other loading conditions the continuum model gives a reasonable representation of a number of properties of the voided material. However, in several different cases the critical strain for localization is considerably overestimated. It is found that these predictions can be much improved by a relatively simple modification of the equations suggested by Gurson. This is particularly noteworthy, because localization is one of the important mechanisms of ductile fracture that is of interest in most applications of the constitutive equations for a voided material.

Descriptions of void nucleation have not been investigated here. However, confidence in the accuracy of the predictions of the void growth model is also important in applications of the Gurson model that accounts for nucleation.

REFERENCES

[1] F.A. McClintock, *Journal of Applied Mechanics* 35 (1968) 363–371.
[2] J.R. Rice and D.M. Tracey, *Journal of the Mechanics and Physics of Solids* 17 (1969) 201–217.
[3] A. Needleman, *Journal of Applied Mechanics* 39 (1972) 964–970.
[4] J.W. Rudnicki and J.R. Rice, *Journal of the Mechanics and Physics of Solids* 23 (1975) 371–394.
[5] H. Yamamoto, *International Journal of Fracture* 14 (1978) 347–365.
[6] V. Tvergaard, *International Journal of Fracture* 17 (1981) 389–407.
[7] A.L. Gurson, *Journal of Engineering Materials and Technology* 99 (1977) 2–15.
[8] A. Needleman and N. Triantafyllidis, *Journal of Engineering Materials and Technology* 100 (1978) 164.
[9] A. Needleman and J.R. Rice, in *Mechanics of Sheet Metal Forming*, eds. D.P. Koistinen *et al.*, Plenum Publishing Corporation (1978) 237–267.
[10] C.-C. Chu, An analysis of localized necking in punch stretching. *MRL E116, Division of Engineering, Brown University* (1979).
[11] C.-C. Chu and A. Needleman, Void nucleation effects in biaxially stretched sheets. *MRL E118, Division of Engineering, Brown University* (1979).
[12] M. Saje, J. Pan and A. Needleman, Void nucleation effects on shear localization in porous plastic solids. Brown University Report, NSF-ENG76–16421/7, June (1980).
[13] R. Hill, *Journal of the Mechanics and Physics of Solids* 6 (1958) 236–249.
[14] C.A. Berg, in *Inelastic Behaviour of Solids*, eds. M.F. Kanninen *et al.*, McGraw-Hill (1970) 171–210.
[15] A.L. Gurson, in *Proceedings of the International Conference on Fracture*, ed. D.M.R. Taplin, 2A, Pergamon Press (1977) 357–364.
[16] V. Tvergaard, *Journal of the Mechanics and Physics of Solids* 24 (1976) 291–304.

RÉSUMÉ

On analyse les propriétés macroscopiques d'un milieu poreux ductile sur base d'un modèle numérique axysimétrique et d'une série d'équations constitutives représentant avec une approximation suffisante un matériau comportant des vides, ainsi que le suggère Gurson. Ces deux modèles sont utilisés pour analyser la biffurcation dans un mode local. Les deux méthodes, qui sont différentes, permettent d'établir plusieurs prédictions qui sont en accord raisonnable. On trouve néanmoins que sous des conditions de charge différentes la déformation critique conduisant à localisation est considérablement surestimée par le modèle d'approximation du continuum. Une modification relativement simple des équations constitutives dans le cas d'un milieu comportant des vides entraîne des prédictions considérablement améliorées.